A Pre-Steady-State Kinetic Analysis of Substrate Binding to Human Recombinant Deoxycytidine Kinase: A Model for Nucleoside Kinase Action†

Boris Turk,‡,§ Raymond Awad,‡ Elena V. Usova,‡ Ingemar Björk,‡ and Staffan Eriksson*,‡

Department of Veterinary Medical Chemistry, Swedish University of Agricultural Sciences, The Biomedical Centre, SE-753 24 Uppsala, Sweden, and Department of Biochemistry and Molecular Biology, J. Stefan Institute, Jamova 39, SI-1000 Ljubljana, Slovenia

Received January 22, 1999; Revised Manuscript Received April 15, 1999

ABSTRACT: Deoxycytidine kinase (dCK) is an enzyme with broad substrate specificity which can phosphorylate pyrimidine and purine deoxynucleosides, including important antiviral and cytostatic agents. In this study, stopped-flow experiments were used to monitor intrinsic fluorescence changes induced upon binding of various phosphate donors (ATP, UTP, and the nonhydrolyzable analogue AMP-PNP) and the acceptor dCyd to recombinant dCK. Monophasic kinetics were observed throughout. The nucleotides as well as dCyd bound to the enzyme by a two-step mechanism, involving a rapid initial equilibrium step, followed by a protein conformational change that is responsible for the fluorescence change. The bimolecular association rate constants for nucleotide binding [$(4-10) \times 10^3$ M^{-1} s^{-1}] were 2−3 orders of magnitude lower than those for dCyd binding [$(1.3-1.5 \times 10^6$ M^{-1} s^{-1}]. This difference most likely is due predominantly to the large difference in the forward rate constants of the conformational changes (0.04−0.26 s^{-1} vs 560−710 s^{-1}). Whereas the kinetics of the binding of ATP, UTP, and AMP-PNP to dCK showed some differences, UTP exhibiting the tightest binding, no significant differences were observed for the binding of dCyd to dCK in the presence or absence of phosphate donors. However, the binding of dCyd to dCK in the presence of ATP or UTP was accompanied by a 1.5- or 3-fold higher quenching amplitude as compared with dCyd alone or in the presence of AMP-PNP. We conclude that ATP and UTP induce a conformational change in the enzyme, thereby enabling efficient phosphoryl transfer.

A number of enzymes are involved in the salvage pathway of nucleosides, with deoxyribonucleoside kinases phosphorylating the deoxyribonucleosides. The newly formed deoxyribonucleoside monophosphates can then be converted to deoxyribonucleoside triphosphates by the sequential action of nucleoside monophosphate kinases and nucleoside diphosphate kinase (*1*). Deoxyribonucleoside kinases are key enzymes of this pathway since they phosphorylate many important anticancer and antiviral drugs, e.g., arabinosylcytosine, 2′-difluorodeoxycytidine, 2-chlorodeoxyadenosine, and 2′,3′-dideoxycytidine (*2*−*6*).

Deoxycytidine kinase (EC 2.7.1.74) catalyzes the 5′-phosphorylation of pyrimidine and purine (deoxy)nucleosides using nucleoside triphosphates as phosphate donors. The enzyme is preferentially expressed in lymphoid cells (*2*, *4*, *6*, *7*), and therefore in earlier investigations lymphoblast or leukemic spleen was used as source for the purifications, which eventually led to pure dCK[1] preparations [reviewed by Arnér and Eriksson (*2*)]. The enzyme is a dimer of two apparently identical 30.5 kDa subunits, and the cloning of dCK cDNA and its subsequent expression in *E. coli* have been described (*7*). In this study we have used the pET vector system for bacterial expression and purification of human dCK (*8*). The purification is based on the presence of an N-terminal histidine tag sequence and metal affinity chromatography (*9*, *10*). A kinetic characterization of the recombinant dCK preparations was done, and the properties were compared to those of the earlier purified dCK from leukemic spleen.

Steady-state substrate kinetic analyses with purified dCK have revealed that the enzyme does not obey Michaelis−Menten kinetics. Instead, bimodal kinetics were obtained with two sets of K_m and V_{max} values (*3*, *4*, *11*). In the case of dCyd, the two apparent K_m values were approximately 1 and 10 μM, whereas the V_{max} value at higher dCyd concentrations was 20−50% higher than that found at low substrate concentrations. The nonlinearity in the saturation curves for various substrates and recombinant dCK was recently reported (*8*); however, the presence of 0.4 M NaCl was shown to alter the kinetic properties of recombinant dCK to

† This work was supported by grants from The Swedish Natural Science Research Council and the Swedish Medical Research Council, by Grant BMH4-CT96-0479 from the EU commission, and in part by the Swedish National Board for Technical Development and Medivir AB, Huddinge, Sweden. B.T. was supported by a fellowship from the Wenner−Gren Foundation and by the Ministry of Science and Technology of Republic of Slovenia.

* Address correspondence to this author at the Department of Veterinary Medical Chemistry, SLU, The Biomedical Centre, Box 575, S-75123 Uppsala, Sweden. Telephone: 4618-471 4187. Fax: 4618-55 07 62. E-mail: Staffan.Eriksson@vmk.slu.se.

‡ Swedish University of Agricultural Sciences.

§ J. Stefan Institute.

[1] Abbreviations: PMSF, phenylmethanesulfonyl fluoride; IPTG, isopropyl-1-thio-β-D-galactopyranoside; DTT, dithiothreitol; dCK, deoxycytidine kinase; AMP-PNP, adenyl imidodiphosphate; PCR, polymerase chain reaction; cDNA, copy DNA; dAdo, 2′-deoxyadenosine; dTTP, deoxythymidine triphosphate; dCTP, deoxycytidine triphosphate.

10.1021/bi990162b CCC: $18.00
Published on Web 06/06/1999

the normal Michaelis−Menten kinetics when dCyd was used as substrate.

Bimodal plots were also obtained when ligand-dependent quenching of dCK intrinsic fluorescence was used to study binding of the substrates to the purified spleen enzyme (*11*). Increasing concentrations of ligands led to decreased fluorescence (approximately 40%) with no change in the peaks of excitation (maximum at 287 nm) and emission (maximum at 332 nm). A relatively low stoichiometry of binding with dCyd, dAdo, dTTP, and the feed-back inhibitor dCTP was observed (0.6−1 molecule of ligand per dimer enzyme). In these earlier fluorescence studies, simultaneous addition of both dCK substrates was not done.

To gain more insight into the mechanism of ligand binding to dCK, a series of pre-steady-state kinetic experiments were performed with recombinant dCK and the substrates dCyd, ATP, the nonhydrolyzable analogue AMP-PNP, and UTP, measuring the changes of dCK intrinsic fluorescence. UTP has been shown to be the preferred phosphate donor for dCK in enzyme kinetic experiments with both pyrimidine and purine deoxynucleosides (*12*−*14*), and it has been suggested that it is the physiological phosphate donor in vivo. These studies lead to new information regarding the steps involved in interactions between dCK and its most important ligands and provide a possible general model for nucleoside kinase action.

MATERIALS AND METHODS

Materials. 2′-[5-^{3}H]Deoxycytidine (32 Ci/mmol) was purchased from Amersham. 2-Chloro-2′-[8-^{3}H]deoxyadenosine (4 Ci/mmol) and 2′-[8-^{3}H]deoxyguanosine (5.8 Ci/mmol) were purchased from Moravek Biochemical Inc. Unlabeled nucleosides, ATP, UTP, and other chemicals were obtained from Sigma Chemical Co. The protease thrombin and Ni^{2+}-NTA−agarose were from Novagen. Ion exchange paper, DE81, was obtained from Whatman. AMP-PNP (adenylyl-imidodiphosphate) was purchased from Boehringer Mannheim.

Construction of pET19b-hdCK and pET9d-hdCK. The human full-length dCK cDNA cloned into pET3d (pET3d-hdCK) (*7*, *10*) was generously provided by B. Mitchell, Department of Pharmacology, University of North Carolina.

To purify recombinant human dCK, Ni^{2+}−agarose chromatography (*9*) was used with the pET19b vector (Novagene), which contains the *Nde*I and *Bam*HI sites for subcloning of the target cDNA. However, there is an *Nde*I site in position 475 of the coding region of human dCK. To circumvent this problem, the partial homology in the recognition sequences for the *Nde*I and *Nco*I restriction enzymes allowed us to change the *Nde*I to an *Nco*I site by using an overlap extension PCR strategy (*15*). The 5′- and 3′-ends of the coding sequence of human dCK were modified by PCR with additional linkers with restriction sites for *Nco*I and *Bam*HI, and the dCK cDNA was ligated into the vector in the same reading frame as the 10-histidine affinity tag and the enterokinase protease site. A pET9d vector (Novagene) construct was also used for expression and purification of recombinant human dCK as described previously (*8*). The fused protein contains in this case a six-histidine affinity tag and a thrombin cleavage site at the N-terminus of the coding sequence.

Expression and Purification of Recombinant dCK. The recombinant dCK constructs (pET9d-hdCK and pET19b-hdCK) were transformed into the pLysS BL21(DE3) host strain (*10*). A single plasmid carrying colony was inoculated in M9ZB growth media containing 50 mg/mL kanamycin and 50 mg/mL chloramphenicol. Expression of the dCK coding DNA was induced by the addition of IPTG, and growth was continued for 4 h at 37 °C. Cells were harvested by centrifugation at 5000 rpm for 10 min at 4 °C, resuspended, and lysed by freeze−thawing and sonication (3 × 1 min) on ice in 20 mM Tris-HCl (pH 7.9), 0.5 M NaCl, and 1 mM PMSF. The lysate was centrifuged at 45 000 rpm (RP 50T-2, LKB Instruments) for 1 h at 4 °C, and dCK was then purified by metal chelate affinity chromatography. The affinity column was washed with a buffer containing 80 mM imidazole, pH 8.0, and 0.5 M NaCl, and dCK was eluted with 0.5 M imidazole in 20 mM Tris-HCl (pH 7.9), 0.5 M NaCl, and 1 mM PMSF. Addition of 10 mM dithiothreitol (DTT) and 20% glycerol to the samples was done directly after elution. The purity of the enzyme was determined by SDS−polyacrylamide gel electrophoresis, and dCK was more than 95% pure using both types of constructs (*8*).

Enzyme Assays. dCK activity was routinely followed by a radiochemical assay procedure as described by Ives et al. (*3*) using the substrates [^{3}H]-dCyd and [^{3}H]-dAdo. Assays were performed in 50 mM Tris-HCl (pH 7.6), 100 mM KCl, 5 mM $MgCl_2$, 5 mM ATP, 2 mM DTT, 0.5 mg/mL BSA, 50 ng of pure dCK, and radiolabeled nucleosides at the concentrations indicated. The reactions were initiated by the addition of enzyme and were terminated by removal of 10 μL aliquots from the reaction mixture, which were spotted onto Whatman DE-81 filter disks at 0, 10, 20, and 30 min. The filter disks were processed and counted as described (*8*).

Analysis of substrate kinetics was done using the Michaelis−Menten and Hill equations and nonlinear regression analysis with the Enzfitter program from Elsever-Biosoft. The two K_m and V_{max} values were derived by using a set of measurements at low and high substrate concentrations (with a range approximately 4-fold lower and higher than the respective K_m values). Kinetic values are from one experiment which has been repeated at least twice with very similar results.

Stopped-Flow Fluorescence Spectroscopy. If not stated otherwise, all kinetic measurements of substrate binding to dCK were done at 25 °C in 0.25 M imidazole, 20 mM Tris-HCl, pH 8.0, containing 0.5 M NaCl, 1 mM EDTA, and 10% (v/v) glycerol. The high ionic strength of the buffer and glycerol were used to stabilize the enzyme.

The kinetics of the phosphate donor (ATP, UTP, AMP-PNP) and dCyd binding to dCK were analyzed in an SX-17MV stopped-flow apparatus (Applied Photophysics, Leatherhead, U.K.) essentially as described earlier (*16*, *17*). Briefly, in the case of phosphate donor binding, one syringe of the stopped-flow apparatus was filled with enzyme and the other with phosphate donor in buffer also containing 10 mM $MgCl_2$. In the case of dCyd binding, one syringe was filled with enzyme and phosphate donor (20 μM final concentration) in buffer containing 10 mM $MgCl_2$ and the other with dCyd in buffer. Data were collected after 5 min incubation time, which was sufficient for temperature equilibration and

Table 1: Steady-State Kinetic Parameters Determined for Three dCK Preparations Using 5 mM ATP as Phosphate Donor and Various Concentrations of [^{3}H]-dCyd or ^{3}[H]-dAdo as Phosphate Acceptor[a]

enzyme	K_{m1} (μM)	K_{m2} (μM)	V_{max1} (nmol/ min^{-1} mg^{-1})	V_{max2} (nmol/ min^{-1} mg^{-1})
dCyd as Substrate				
spleen dCK	0.6	7	61	72
pET9d-hdCK	1.7	3	80	130
pET19b-hdCK	1.0	3.4	240	430
dAdo as Substrate				
spleen dCK	65	1400	180	542
pET9d-hdCK	27	106	441	872
pET19b -hdCK	50	560	460	1200

[a] Data for the spleen enzyme are from Bohman (*18*) and the recombinant enzymes contained the histidine tag sequence. The values are from one typical experiment which has been repeated twice with very similar results.

in the latter case also for completion of phosphate donor binding to dCK (see Results). Reactions were monitored by the change in tryptophan fluorescence emission accompanying the interaction at an excitation wavelength of 285 nm and with an emission cutoff filter with ~50% transmission at 320 nm. The absorbances at the excitation wavelength for the highest nucleotide concentrations used corresponded to inner-filter effects of ≤18%. At least a 10-fold molar ratio of ligands to dCK was used throughout.

RESULTS

Characterization of Pure Recombinant dCK Preparations. Initially the pET3d-hdCK was used for bacterial expression of human dCK (*7*). The disadvantage with this type of vector is that the purification is relatively complicated, and therefore we tested other vector systems that allow N-terminal fusion of cleavable His-Tag sequences for rapid affinity purification. The pET19b vector containing a 10-histidine affinity tag and an enterokinase protease cleavage site was used. The cleavage of purified dCK left an additional histidine originating from the protease site at the N-terminus of the protein. Due to the absence of a suitable cloning site in the vector, an alternate cloning and mutagenesis procedure (*15*) had to be used to insert the cDNA in-frame in the pET19b vector (see Materials and Methods).

Induction of pET19b-hdCK transfected bacteria, preparation of extracts, and subsequent purification on Ni^{2+}-agarose columns have been done as described by the suppliers. Preparations of pure dCK were stable in the elution buffer at −70 or −20 °C, but lost approximately 50% of the activity after 2 weeks storage at 4 °C. Freezing and thawing led to inactivation, and therefore we routinely kept the enzyme at −20 °C in the presence of 20% glycerol and 10 mM DTT. Removal of the histidine tag sequence from pET19b-hdCK was done using enterokinase. This first required dialysis to exchange the buffer and then an incubation with 2% enterokinase for 36 h at 25 °C in order to get more than 90% digestion of the fusion protein. The digested dCK preparation showed about 50% lower specific activity and higher K_m values (data not shown) as compared to undigested enzyme, and therefore uncleaved dCK was in most cases used in the kinetic studies.

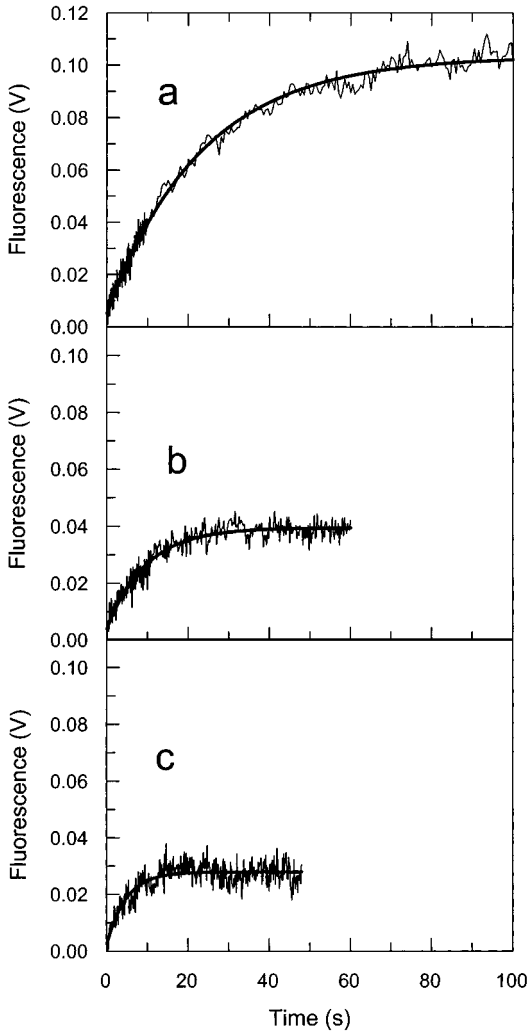

FIGURE 1: Kinetics of binding of nucleotides to dCK at 25 °C and pH 8.0. The increase of tryptophan fluorescence accompanying the interaction was monitored as descibed under Materials and Methods. (a) UTP binding; (b) ATP binding; (c) AMP-PNP binding. The dCK concentration was 2 μM in all three experiments, whereas UTP, ATP, and AMP-PNP concentrations were 0.125 mM, 0.6 mM, and 1 mM, respectively. The solid lines are the theoretical curves corresponding to the best fits to a single-exponential function obtained by nonlinear regression analysis: k_{obs} = 0.043 s^{-1}, amplitude = 98 mV (a); k_{obs} = 0.098 s^{-1}, amplitude = 39 mV (b); k_{obs} = 0.21 s^{-1}, amplitude = 26 mV (c). The amplitudes and the rate constants were determined at a single reactant concentration.

In the case of the pET9d bacterial vector system, where the recombinant human dCK contains a six-histidine tag and a thrombin cleavage site, we found that the histidine tag could be effectively removed using thrombin cleavage at 10 °C for 30 h. This resulted in a pure dCK preparation with three additional amino acids: Gly, Ser, and Ala at the N-terminus (*8*). Addition of 10 mM dithiothreitol and 20% glycerol stabilized the enzyme, and a detailed kinetic analysis of the pET9d-dCK could be done as well as fluorescence studies as described below.

It was important to know if alteration of the N-terminus of dCK as a result of the fusion of the histidine tag and protease sites influenced the kinetic behavior. We therefore tested two different recombinant dCK constructs, pET9d-hdCK and pET19b-hdCK, with dCyd and dAdo as substrates. The kinetic results obtained were compared with the results from the spleen enzyme and were similar for both types of

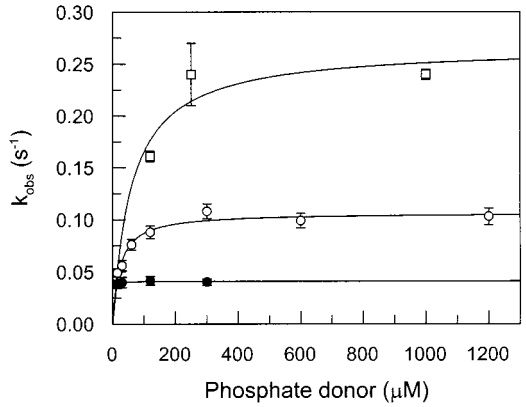

FIGURE 2: Dependence of k_{obs} on nucleotide concentration for binding to dCK. Filled circles, UTP; open circles, ATP; open squares, AMP-PNP. Average values, determined as detailed under Materials and Methods, are shown together with their standard errors. Error bars not shown lie within the dimensions of the symbols. Solid lines represent the best fits to eq 1 (Table 2), with k_{-2} values set to 0.

dCK preparations (Table 1 and not shown). The V_{max} and K_m values of the pET9d dCK preparations with dCyd are relatively similar to those of the purified spleen dCK (6, 18), but the K_m values are somewhat lower and the V_{max} values 3-fold higher in the case of pET19b-hdCK. The activity with dAdo as substrate is also higher with the recombinant enzyme as compared with the spleen enzyme. The reasons for these differences are not known but may be related to the rapid purification procedure and differences in the protein folding process. The kinetic results were very similar with protease-treated and untreated recombinant dCK (data not shown), indicating that the histidine tag sequence had little effect on the substrate interactions.

Pre-Steady-State Kinetics of Phosphate Donor Binding to Recombinant dCK. A series of pre-steady-state experiments were performed using stopped-flow equipment with recombinant dCK and various phosphate donors. The results were essentially identical with both of the recombinant dCK preparations described above. The interaction of ATP, UTP, and the nonhydrolyzable analogue AMP-PNP with dCK resulted in an increase of intrinsic enzyme fluorescence, which could be best described by a single-exponential function in the whole concentration range studied (Figure 1). The amplitudes, corrected for the inner-filter effects, observed for UTP binding (95 ± 5 mV; average of four concentrations) were almost 2-fold higher than those for ATP binding (53 ± 6 mV; average of four concentrations) and 4-fold higher than those for AMP-PNP binding (26 ± 1 mV; average of two concentrations), all at saturating concentrations of the ligands. This result indicated that the three nucleotides bind somewhat differently to the enzyme. Increasing ATP concentration resulted in a hyperbolical increase of k_{obs} (the observed pseudo-first-order rate constant) as shown in Figure 2. This behavior is consistent with a two-step process involving a rapid initial equilibrium step, followed by a protein conformational change, which is responsible for the fluorescence change. In contrast, the data are not consistent with the alternative two-step mechanism, in which an enzyme conformational change precedes substrate binding, as this mechanism is characterized by a decrease in the rate constant with increasing substrate concentrations (*19*). The applicable mechanism is shown in the following scheme:

Table 2: Kinetic Constants for Nucleotide Binding to dCK at 25 °C and pH 8.0[a]

nucleotide	K_1 (μM)	k_{+2} (s^{-1})	k_{on} (M^{-1} s^{-1})
AMP-PNP	61 ± 24[b]	0.27 ± 0.02	4400 ± 2100[b]
ATP	22 ± 4	0.11 ± 0.004	4800 ± 1000
UTP	<5.0[b]	0.041 ± 0.001	>38000[b]

[a] The dissociation equilibrium constant for the first step (K_1) and the forward rate constant for the second step (k_{+2}) of Scheme 1 were obtained by nonlinear regression analysis of eq 1 to the experimental data in Figure 2. Bimolecular association rate constants (k_{on}) were calculated from the values of K_1 and k_{+2} ($k_{on} = k_{+2}/K_1$). All errors represent ±SE. [b] Approximate values.

Scheme 1

$$\text{dCyd} + \text{dCK} \underset{k_{+2}}{\overset{K_1}{\rightleftharpoons}} \text{dCyd}-\text{dCK} \underset{k_{-2}}{\overset{k_{+2}}{\rightleftharpoons}} \text{dCyd}-\text{dCK}^*$$

where K_1 represents the equilibrium dissociation constant of the initial binding step k_2 and k_{-2} represent the forward and reverse rate constants of the conformational change (denoted by an asterisk). According to this scheme, k_{obs} is given by the following equation (*20*):

$$k_{obs} = \frac{k_{+2}[S]_0}{K_1 + [S]_0} + k_{-2} \quad (1)$$

where $[S]_0$ represents the initial substrate concentration. Whereas the values of k_{+2} and K_1 could be determined with good or moderate precision (Table 2), respectively, only an estimate could be made for the value of k_{-2} (~0.01 s^{-1}). There are two main reasons for this: (i) lower saturation of the enzyme at low concentrations of ATP, which resulted in a smaller signal change approaching the detection limit; and (ii) prolonged duration of experiments, which could have resulted in photodecomposition of the enzyme. These were also the main reasons that binding of AMP-PNP and UTP could only be followed in a limited concentration range, which enabled us to determine k_{+2} values only (Table 2). The K_1 values for these two analogues shown in Table 2 are therefore only approximate, and no k_{-2} values at all could be obtained.

Pre-Steady-State Kinetics of dCyd Binding to Recombinant dCK. Earlier studies with purified spleen dCK demonstrated substrate-induced quenching of the intrinsic trypthophan fluorescence of the enzyme. Initial steady-state spectrofluorometric analyses of pure pET19b-hdCK with dCyd, dAdo, arabinosylcytosine, and 2-chlorodeoxyadenosine (at concentrations approximately 2 times their K_{m1} values) gave similar results, although the quenching of intrinsic fluorescence was on the average somewhat lower (10−15%, data not shown) than those values reported earlier (*11*).

Binding of dCyd to dCK in the absence or presence of various phosphate donors (AMP-PNP, ATP, UTP) was monitored by stopped-flow fluorescence under pseudo-first-order conditions. The kinetics of fluorescence change for all combinations were monophasic in the whole concentration range studied and could be best fitted to a single-exponential function (Figure 3). The fluorescence amplitudes were markedly different (Figure 3). Whereas they were practically identical in the absence of phosphate donors (200 ± 4 mV)

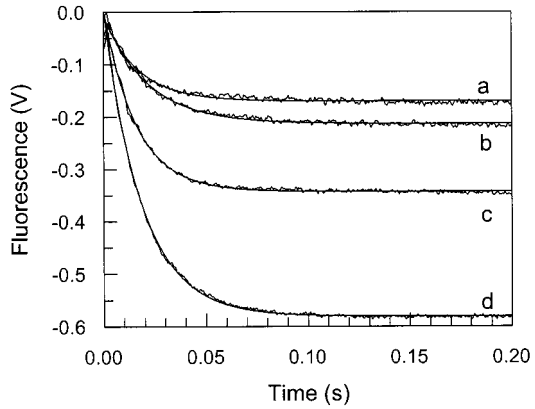

FIGURE 3: Kinetics of binding of dCyd to dCK, preincubated with various nucleotides at 25 °C and pH 8.0. The decrease of tryptophan fluorescence accompanying the interaction was monitored as descibed under Materials and Methods. (a) dCK + AMP-PNP; (b) dCK alone; (c) dCK + ATP; (d) dCK + UTP. dCyd and dCK concentrations were 45 and 2 μM, respectively. All the nucleotides were used at 20 μM final concentration. The solid lines are the theoretical curves corresponding to the best fits to a single-exponential function obtained by nonlinear regression analysis; (k_{obs} = 58.8 s^{-1}, amplitude = 170 mV (a); k_{obs} =51.4 s^{-1}, amplitude = 200 mV (b); k_{obs} = 60.4 s^{-1}, amplitude = 350 mV (c); k_{obs} = 54.7 s^{-1}, amplitude = 590 mV (d).

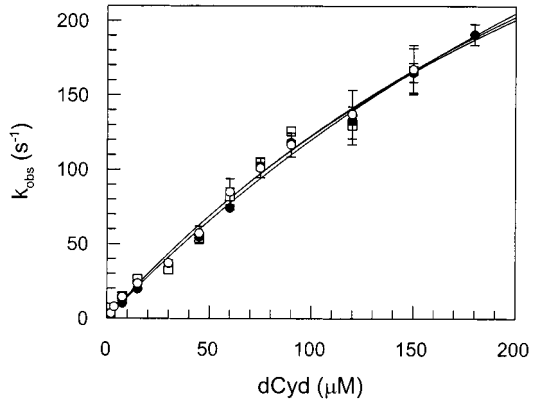

FIGURE 4: Dependence of k_{obs} on dCyd concentration for binding to dCK−nucleotide complexes. Filled circles, dCK−UTP; open circles, dCK-ATP; open squares, dCK alone. Average values, together with their standard errors, were determined as detailed under Materials and Methods. Error bars not shown lie within the dimensions of the symbols. Solid lines represent the best fits to eq 1 (Table 3).

and in the presence of AMP-PNP (170 ± 5 mV), the amplitude in the presence of ATP was ~1.5-fold higher (350 ± 10 mV) than the former and that in the presence of UTP almost 3-fold higher (590 ± 8 mV). In these experiments, inner filter corrections were negligible (≤5%). Increasing the ATP concentration from 20 μM to 180 and 600 μM did not increase the amplitude, indicating that dCK was saturated with the phosphate donor. Similar results were also obtained with the other phosphate donors, although the concentration range tested was lower (20−125 μM for both UTP and AMP-PNP), which in the latter case may not be saturating.

The dependence of the observed pseudo-first-order constants, k_{obs}, on dCyd concentrations was studied in the absence of phosphate donors or in the presence of ATP and UTP (Figure 4). As was observed for phosphate donor binding, k_{obs} increased hyperbolically with increasing substrate concentration, $[S]_0$, in all cases, although the high-k_{obs} values prevented measurements close to saturation. This hyperbolic dependence again indicated a two-step process (Scheme 1). Equation 1 describing this mechanism could be well fitted to all three data sets by nonlinear regression analysis. The experimental data points for the different combinations overlapped each other, which is also reflected in the highly similar kinetic constants (Table 3).

Table 3: Kinetic Constants for dCyd Binding to dCK, Complexed with Various Phosphate Donors, at 25 °C and pH 8.0[a]

nucleotide	K_1 (μM)	k_{+2} (s^{-1})	k_{on} (M^{-1} s^{-1})
none	350 ± 160	560 ± 200	1.3 ± 0.1
ATP	380 ± 80	590 ± 90	1.5 ± 0.2
UTP	490 ± 130	710 ± 150	1.3 ± 0.1

[a] The dissociation equilibrium constant for the first step (K_1) and the forward rate constant for the second step (k_{+2}) of Scheme 1 were obtained by nonlinear regression analysis of eq 1 to the experimental data in Figure 4. Bimolecular association rate constants (k_{on}) were calculated from the slopes of the linear portions of the plots of k_{obs} vs dCyd concentration (2−60 mM dCyd). All errors represent ± SE.

At lower dCyd concentrations, k_{obs} values showed a linear dependence on dCyd concentration, providing the second-order association rate constants, k_{on} (=k_2/K_1; Table 3). However, the intercepts were experimentally indistinguishable from the origin, thus precluding the determination of dissociation rate constants, k_{-2}, although an upper limit of ~2 s^{-1} could be estimated for k_{-2} from the plots. From this value, an upper limit for K_d of ~1.5 μM ($K_d = k_{off}/k_{on}$) could be estimated for the binding of dCyd to dCK in the presence or absence of phosphate donors, which is in agreement with a previous steady-state study (*11*).

DISCUSSION

Conformational changes are important parts of the catalytic mechanisms of a number of enzymes (*21*). Several kinases, e.g., nucleoside monophosphate kinases (*22*, *23*), phosphoglycerate kinases (*24*, *25*), GTP-binding proteins (protein kinases) (*26*, *27*), and other nucleotide binding proteins such as GroEL chaperonins (*28*−*30*), all exhibit pronounced domain movements upon nucleotide binding. As was shown for adenylate kinase, the best studied nucleoside monophosphate kinase, the conformational changes were observed not only during binary complex formation but also during binary-to-ternary complex formation (*31*, *32*).

Although no structural data are available for any of the cellular deoxynucleoside kinases, the intrinsic fluorescence changes accompanying substrate binding to dCK are likely to reflect such conformational rearrangements. The two-step mechanisms for both nucleotide and dCyd binding to dCK demonstrated here are in agreement with the two-step mechanism observed for ligand binding to nucleoside diphosphate kinase (*33*) and with the multiple conformational changes observed with adenylate kinase (*23*), suggesting that dCK exhibits a similar binding mechanism as the other kinases.

A kinetic comparison between UTP, ATP, and AMP-PNP binding to dCK showed individual differences. The rate constant for the conformational change induced by UTP was ~2-fold and ~4-fold lower than to those for ATP and AMP-PNP binding, respectively (Table 2). However, the bimolecular association rate constant, k_{on}, for UTP binding was the highest (38 000 M^{-1} s^{-1}) as a result of a tighter initial complex formation (K_1 < 5 μM). The k_{on} values for ATP

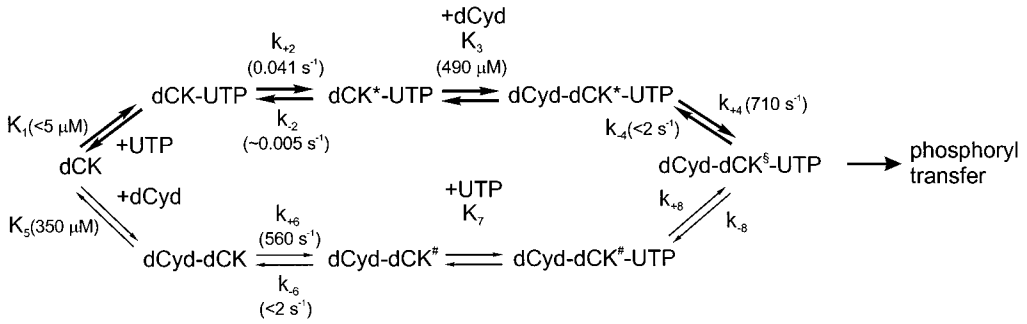

FIGURE 5: Schematic model for the mechanism of ligand binding to dCK. The major (kinetically preferred) pathway is marked with thick arrows and the minor with thin arrows.

and AMP-PNP binding were similar (4800 vs 4400 M^{-1} s^{-1}) due to a weaker initial binding of ATP and AMP-PNP. This is in agreement with previous results, where UTP was shown to bind to dCK with a higher affinity than the other phosphate donors (*34*). Although a k_{-2} value for UTP could not be determined from the intercept of the k_{obs} vs $[S]_0$ plots, it was possible to get an estimate of this parameter based on the K_i value, which should be similar to the K_d value (*34*, *35*). A k_{-2} value of ~0.005 s^{-1} could be calculated in this way from a K_i of 0.6 μM (*34*). However, a similar calculation gave a k_{-2} of 0.28 s^{-1} for ATP−dCK binding [K_i= 60 μM (*34*)], which is substantially higher than the k_{-2} (~0.01 s^{-1}) estimated from the data in Figure 2, suggesting that the true K_d value for the ATP−dCK interaction is considerably lower. In agreement with this conclusion, recent experiments using quenching of the intrinsic fluorescence of recombinant dCK under steady-state conditions gave a monophasic binding curve for ATP with a K_d of 8.4 μM (*36*).

Contrary to the nucleotide binding results, the kinetics of dCyd binding to dCK−nucleotide complexes or to dCK alone were experimentally indistinguishable. However, there are likely differences in the k_{-2} values, indicated by the lower K_m values obtained by steady-state studies in the presence of UTP (0.15−0.5 μM) than in the presence of ATP (0.8−1.0 μM) (*14*, *34*). Despite the similarity of the kinetic properties, the fluorescence amplitudes accompanying binding of the two phosphate donors were markedly different (Figure 3). The large changes observed in the presence of both true substrates (dCyd and UTP/ATP), which are larger than the sum of the individual contributions of the substrates, suggest that both substrates contribute to catalytically important conformational changes, as was also observed with phosphoglycerate kinase (*37*). Moreover, these results indicate the formation of ternary complexes between dCK, dCyd, and UTP or ATP, confirming a previous suggestion by Hughes et al. (*34*). Since UTP has been shown to be a more efficient phosphate donor than ATP (*12*−*14*, *34*), the higher amplitudes observed for dCyd binding to dCK in the presence of UTP are most likely a consequence of a somewhat different conformational change induced by dCyd binding to the UTP−dCK complex. This conformational change apparently allows tighter substrate binding, possibly enabling a more efficient phosphoryl transfer. This hypothesis is supported by the finding that AMP-PNP, which is an ATP analogue unable to perform phosphoryl transfer, did not induce this type of conformational change. Similar results were obtained with the ATP-binding protein GroEL/GroES chaperone, for which crystallographic studies with ATP and two different nonhydrolyzable analogues, AMP-PNP and ATP-γS, bound to the chaperone showed clearly different and much smaller conformational changes induced by the nonhydrolyzable nucleotides (*30*, *38*).

Nucleotides, especially UTP, were found to interact with dCK with a higher or similar affinity as dCyd (*34*), and it was therefore surprising that nucleotide binding was substantially slower (2−3 orders of magnitude) than dCyd binding. This was mainly a consequence of the very low rate constant for the conformational change (0.04−0.26 s^{-1} vs 560−710 s^{-1}) and only partially compensated for by the lower K_1 values for nucleotide binding. The higher affinity of nucleotides for dCK is therefore a consequence of substantially higher stabilities of the final nucleotide−dCK complexes, which is reflected in the very low rate constants for the reversal of the conformational change.

Based on these and previous results (*39*, *34*, *36*), a model for dCK action can be proposed (Figure 5). In this model, the majority of phosphoryl transfer is accomplished via UTP binding to dCK before dCyd binding. Although dCyd can bind to dCK faster than the nucleotides even at physiological conditions ([dCyd] ≅ 20 μM, [UTP] ≅ 0.8 mM) due to the much higher k_{on}, the majority of the dCyd molecules would dissociate from dCK prior to nucleotide binding as a result of a very high k_{off} value. Only a minor portion of the phosphoryl transfer can thus be accomplished by binding of dCyd prior to the binding of the phosphate donor. UTP binding induces a conformational change in dCK, and contrary to the unstable dCyd−dCK# complex, such a UTP−dCK* complex is stable and kept in a conformation favorable for phosphoryl transfer (=activated complex), as judged by the different amplitudes of dCyd binding to dCK and to the dCK−nucleotide complexes. In the next step, a ternary complex is formed between dCyd and the activated complex (UTP−dCK*), followed by additional conformational rearrangement (dCyd−dCK§−UTP) and subsequent phosphoryl transfer. The model is further supported by the finding that the kinetics of dCyd binding to dCK or dCK−nucleotide complexes are indistinguishable, indicating that dCyd can randomly bind to dCK and UTP−dCK*, providing evidence for the two branches of the reaction pathway. Although the conformational change in the protein is the most likely mechanism, we cannot exclude the possibility that the substrate has undergone some conformational rearrangement. Since all nucleoside kinases studied so far exhibit substrate-induced conformational changes, we suggest that a mechanism like the one presented could be a general model for the action of nucleoside kinases. This type of dynamic behavior cannot be defined by crystallographic studies but can be analyzed in detail with pre-steady-state kinetic experiments.

ACKNOWLEDGMENT

We thank Liya Wang for constructing the pET-9d and pET-19b-hdCK vectors.

REFERENCES

1. Reichard, P. (1988) *Annu. Rev. Biochem. 57*, 349−374.
2. Arnér, E. S. J., and Eriksson, S. (1995) *Pharmacol. Ther. 67*, 155−186.
3. Ives, D. H., and Durham, J. P. (1970) *J. Biol. Chem. 245*, 2285−2294.
4. Sarup, J. C., and Fridland, A. (1987) *Biochemistry 26*, 590−597.
5. Krenitsky, T. A., Tuttle, J. V., Koszalka, G. W., Chen, I. S., Beacham, L., Rideout, J. L., and Elion, G. B. (1976) *J. Biol. Chem. 251*, 4055−4061.
6. Bohman, C., and Eriksson, S. (1988) *Biochemistry 27*, 4258−4265.
7. Chottiner, E. G., Shewach, D. S., Datta, N. S., Ashcraft, E., Gribbin, D., Ginsburg, D., Fox, I. H., and Mitchell, B. S. (1991) *Proc. Natl. Acad. Sci. U.S.A. 88*, 1531−1535.
8. Usova, E. V., and Eriksson, S. (1997) *Eur. J. Biochem. 248*, 762−766.
9. Petty, K. J. (1993) *Curr. Protocols Mol. Biol.* Suppl. 24, 10.11.8.
10. Studier, F. W., Rosenberg, A. H., Dunn, J. J., and Dubendorff, J. W. (1990) *Methods Enzymol. 185*, 60−89.
11. Kierdaszuk, B., Rigler, R., and Eriksson, S. (1993) *Biochemistry 32*, 699−707.
12. White, J. C., and Capizzi, R. L. (1991) *Cancer Res. 51*, 2559−2565.
13. Shewach, D. S., Reynolds, K. K., and Hertel, L. (1992) *Mol. Pharmacol. 42*, 518−524.
14. Krawiec, K., Kierdaszuk, B., Eriksson, S., Munch-Petersen, B., and Shugar, D. (1995) *Biochem. Biophys. Res. Commun. 216*, 42−48.
15. Ho, S. N., Hunt, H. D., Horton, R. M., Pullen, J. K., and Pease, L. R. (1989) *Gene 77*, 51−59.
16. Turk, B., Colic, A., Stoka, V., and Turk, V (1994) *FEBS Lett. 339*, 155−159.
17. Turk, B., Stoka, V., Björk, I., Boudier, C., Johansson, G., Dolenc, I., Colic, A., Bieth, J. G., and Turk, V. (1995) *Protein Sci. 4*, 1874−1880.
18. Bohman, C. (1989) Doctoral Thesis, The Karolinska Institute, Stockholm.
19. Fersht, A. (1999) in *Structure and Mechanism in Protein Science: A Guide to Enzyme Catalysis and Folding*, pp 147−149, W. H. Freeman and Company, New York.
20. Olson, S. T., Halvorson, H. R., and Björk, I. (1991) *J. Biol. Chem. 266*, 6342−6352.
21. Gerstein, M., Lesk, A. M., and Chothia, C. (1994) *Biochemistry 33*, 6739−6749.
22. Vonrheim, C., Schlauderer, G. J., and Schulz, G. E. (1995) *Structure 3*, 483−490.
23. Muller, C. W., Schlauderer, G. J., Reinstein, J., and Schultz, G. E. (1996) *Structure 4*, 147−156.
24. Banks, R. D., Blake, C. C. F., Evans, P. R., Haser, E., Rice, D. W., Hardy, G. W., Merett, M., and Philips, A. W. (1979) *Nature 279*, 773−777.
25. Watson, H. C., Walker, N. P., Shaw, P. J., Bryant, T. N., Wendell, P. L., Fothergill, L. A., Perkins, R. E., Conroy, S. C., Dobson, M. J., Tuite, M. F., Kingsman, A. J., and Kingsman, S. M. (1982) *EMBO J. 1*, 1635−1640.
26. Pai, E. F., Krengel, U., Petsko, G. A., Goody, R. S., Kabsch, W., and Wittinghofer, A. (1990) *EMBO J. 9*, 2351−2359.
27. Coleman, D. E., Berghuis, A. M., Lee, E., Linder, M. E., Gilman, A. G., and Sprang, S. R. (1994) *Science 265*, 1405−1412.
28. Braig, K., Otwinowski, Z., Hegde, R., Boisvert, D. C., Joachimiak, A., Horwich, A. L., and Sigler, P. B. (1994) *Nature 371*, 578−586.
29. Boisvert, D. C., Wang, J., Otwinowski, Z., Horwich, A. L., and Sigler, P. B. (1996) *Nat. Struct. Biol. 3*, 170−177.
30. Roseman, A. M., Chen, S., White, H., Braig, K., and Saibil, H. R. (1996) *Cell 87*, 241−251.
31. Pal, P. K., Ma, Z., and Coleman, P. S. (1992) *J. Biol. Chem. 267*, 25003−25009.
32. Sinev, M. A., Sineva, E. V., Ittah, V., and Haas, E. (1996) *Biochemistry 35*, 6425−6437.
33. Schneider, B., Xu, Y. W., Sellam, O., Sarfati, R., Janin, J., Veron, M., and Deville-Bonne, D. (1998) *J. Biol. Chem. 273*, 11491−11497.
34. Hughes, T. L., Hahn, T. M., Reynolds, K. K., and Shewach, D. S. (1997) *Biochemistry 36*, 7540−7547.
35. Li, Y., Zhang, Y., and Yan, H. (1996) *J. Biol. Chem. 271*, 28038−28044.
36. Shafiee, M., Gosselin, G., Imbach, J.-L., Divita, G., Eriksson, S., and Maury, G. (1998) *Eur. J. Med. Chem.* (in press).
37. Cheung, C. W., and Mas, M. T. (1996) *Protein Sci. 5*, 1144−1149.
38. Llorca, O., Marco, S., Carrascosa, J. L., and Valpuesta, J. M. (1994) *FEBS Lett. 345*, 181−186.
39. Kim, M.-Y., and Ives, D. H. (1989) *Biochemistry 28*, 9043−9047.

BI990162B